

Design of Frequency Selective Surface (FSS) for 6G communications

<http://www.doi.org/10.62341/2059>

Wafaa Ahmad Gbreil¹, Sumia Younes Saleh², Wafa Alsadik Hammad³, Shahid Salim
Mohammed⁴, Azhar Idris Alfarjani⁵, Nuhay Murajia Sulayman⁶

Department of Electrical Engineering Faculty of Engineering University of Benghazi
Wafaa.hamd@uob.edu.ly

Abstract

We propose a quartz-supported frequency selective surface (FSS) for 6G communication, featuring a gear-shaped metallic array on a single layer. The transmission characteristics are investigated using full-wave simulation and the equivalent circuit method. Additionally, the surface current distribution, electric field, and magnetic field distributions are studied to better understand the transmission mechanism. The simulation results show that a resonant frequency of 16.63 GHz can be achieved with an attenuation of -80 dB. The transmission response of the FSS prototype was measured using a free space setup, and the measured results matched well with the simulated ones, confirming the design and fabrication reliability. The proposed FSS, with its simple structure, low cost, easy fabrication, and integration advantages, can enhance communication performance and anti-interference capabilities in future 6G system.

Keywords: 6G; communication; frequency selective surface; circular loop; Transmission; Square Loop.

تصميم سطح انتقائي للترددات المقترحة لاتصالات الجيل السادس

وفاء أحمد جبريل¹ سميه يونس² وفاء الصادق حماد³
شهد سالم محمد⁴ أزهار ادريس الفرجاني⁵ نهى امرجس سليمان⁶

جامعة بنغازي كلية الهندسة قسم الهندسة الكهربائية والإلكترونية

الملخص

تم اقتراح سطح انتقائي للتردد مدعوم بالكوارتز (FSS) للاتصالات الجيل السادس، يتميز بمصفوفة معدنية على شكل ترووس على طبقة واحدة. تم فحص خصائص الإرسال باستخدام محاكاة الموجة الكاملة وطرق الدائرة المكافئة. كما تم فحص توزيعات التيار السطحي والمجال الكهربائي والمغناطيسي لفهم آلية الإرسال بشكل أفضل. وأظهرت نتائج المحاكاة أنه يمكن الحصول على تردد رنين يبلغ 16.63 جيجا هرتز مع توهين بمقدار - 80 ديسيبل، وتم قياس استجابة الإرسال للنموذج الأولي لجهاز FSS باستخدام إعداد الفضاء الحر، وتتفق النتائج المقاسة بشكل جيد مع نتائج المحاكاة، مما يؤكد موثوقية التصميم. ويتميز جهاز FSS المقترح بمزايا الهيكل البسيط والتكلفة المنخفضة، ويمكنه تحسين أداء الاتصالات والقدرة على منع التداخل في أنظمة الجيل السادس المستقبلية.

الكلمات المفتاحية: الجيل السادس ، اتصالات ، تردد سطح انتقائي ، حلقة دائرية ، الإرسال ، حلقة مربعية .

1.Introduction

With the commercialization of 5G communication technology, research on 6G [7] technology is underway to achieve higher data rates and lower latency. The most promising frequency range for 6G communication is between 7-20 [1], due to considerations of power source and system integration. As a result, there is a growing demand for devices such as absorbers, antennas[2,5,6], filters[3,4], and lenses that meet the requirements of being low-cost, simple in structure, compact, and highly integrated Frequency Selective Surface (FSS) [12] is a solution that meets these requirements and has been widely used in various applications including filters, antenna reflectors, radomes, absorbers, and electromagnetic (EM) applications. Indeed, these frequency selective surfaces have several performance advantages for their application areas. For example, designed frequency selective surfaces [8] have better polarization stability due to the use of hexagonal cavities. Of course, this makes their construction and fabrication somewhat complex: the frequency-selective surface reported in [9] can provide a flat passband. The frequency-selective surface proposed in [10] can provide a four-band frequency response, is limited by its large thickness for many applications. The frequency-selective surface in [11] has a structure. On the other hand, its performance is a bit weaker. There a balance must be struck between structural complexity, thickness, and manufacturing. The FSS proposed in this paper operates at a resonant frequency of 16.63 GHz, making it suitable for the frequency range expected to be used in 6G communication.

This FSS features a simple structure with a single-layer design of gear-shaped metal arrays deposited on quartz glass, making it cost-effective and easy to fabricate. It provides excellent filtering capabilities while striking a balance between structure complexity, thickness, and fabrication requirements. The simulations are done using CST Microwave Studio.

2. Structure, Analysis, and Discussion

The FSS structure consists of a two-dimensional periodic array of circular loops. The geometry of the FSS being studied is shown in Fig.1. Each unit cell contains a printed circular conducting loop. A thin substrate layer is used to aid in the fabrication of the FSS for printing the conducting loops. The substrate has a thickness (h) and relative permittivity (ϵ) that should be kept to a minimum. The equivalent circuit model (ECM) of the circular loop FSS is shown in Fig.2, which includes a LC circuit where the inductance (L) and capacitance (C) are represented by the conducting elements and inter-element spacing, respectively. Therefore, the resonant frequency can be determined as:

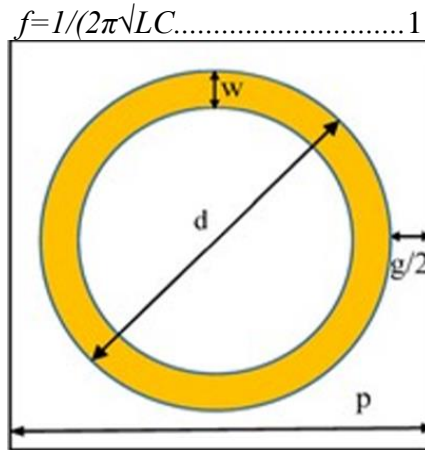


Figure 1: The geometry circular loop FSS

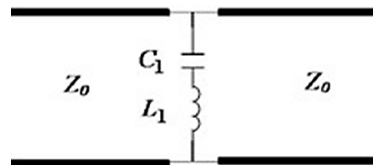


Figure 2: LC circuit

The proposed single-layer FSS is simulated and optimized using CST Microwave Studio software. These parameters were as follows in table 1.

Table 1: Dimensions of the design

X	Y	met_h	w	r_out	Sub_h
14	14	0.035	0.5	6	0.5

The difference between the upper and lower frequency responses at-10 dB represents the fractional bandwidth:

$$\text{Bandwidth} = \frac{f_u - f_l}{f_0} \times 100\% \dots \dots \dots 2$$

The circuit model for oblique angles of incidence necessitates the inclusion of inductance and capacitance expressions for both transverse electric (TE) and transverse magnetic (TM) incidence. By utilizing the geometry depicted in the fig3, the fundamental equations for determining the inductance and capacitance of strip gratings with periodicity (p), width, and spacing (g) at oblique angles of incidence can be derived from, and the overall forms are provided by[13]

$$X_{TE} = F(p, w, \lambda, \theta) = \frac{p \cos \theta}{\lambda} \left[\ln \left(\csc \frac{\pi w}{2p} \right) + G(p, w, \lambda, \theta) \right] \dots \dots \dots 3$$

$$B_{TM} = 4F(p, g, \lambda, \phi) = \frac{4p \cos \theta}{\lambda} \left[\ln \left(\csc \frac{\pi g}{2p} \right) + G(p, g, \lambda, \phi) \right] \dots \dots \dots 4$$

$$X_{TM} = \frac{p \sec \phi}{\lambda} \left[\ln \left(\csc \frac{\pi w}{2p} \right) + G(p, w, \lambda, \phi) \right] \dots \dots \dots 5$$

$$B_{TE} = \frac{4p \sec \theta}{\lambda} \left[\ln \left(\csc \frac{\pi g}{2p} \right) + G(p, g, \lambda, \theta) \right] \dots \dots \dots 6$$

Where θ and ϕ are the angles of incidence, λ is the wavelength, and G is the correction term started i. By varying θ and ϕ , it allows incidence of the plane waves at arbitrary angled. Langley and parker have extracted the lumped-element ECM for the square-loop array. Accordingly, a lumped-element ECM can be obtained for circular loop array.

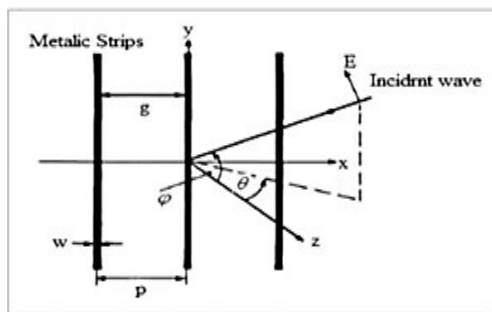


Figure 3: Plane wave incidence upon an inductive Strip grating. For a capacitive strip grating, replace the incident electric field (E) with a magnetic field (H)

3. SIMULATION RESULTS

The proposed FSS was designed and simulated using CST software in fig4. The simulation included unit cell boundaries, and the corresponding transmission coefficients for TE mode and TM mode were shown in Fig.5 and Fig.6, respectively From Fig.5, it can be observed that a return loss of less than -80dB indicates that in the stop band, no signal passes through. This means that the frequency range from 15.36 GHz to 17.14 GHz

is blocked by the FSS structure, with a resonance peak occurring at 16.63 GHz. The stop band FSS structure allows frequencies below 15.36 GHz and above 17.14 GHz to pass through. On the other hand, the band pass FSS structure permits frequencies between 8.55 GHz and 17.47 GHz to pass through, while blocking frequencies below 8.55 GHz and above

17.45 GHz. It is worth noting that the resonance for the pass or stop band occurs at the same frequency, which is 16.76 GHz.

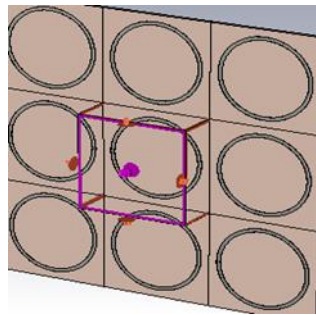


Figure 4: Unit cell boundary

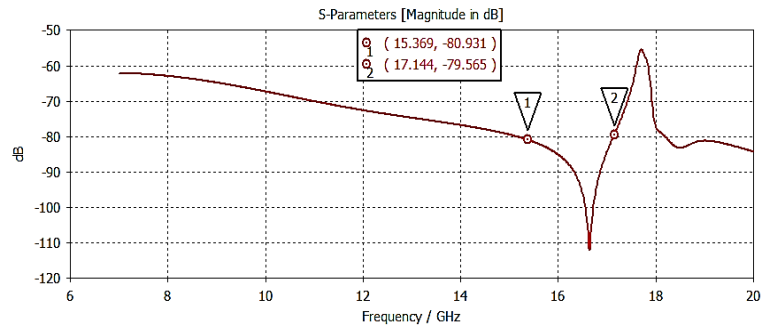


Figure 5: Transmission parameters (stop band) for TE and TM mode

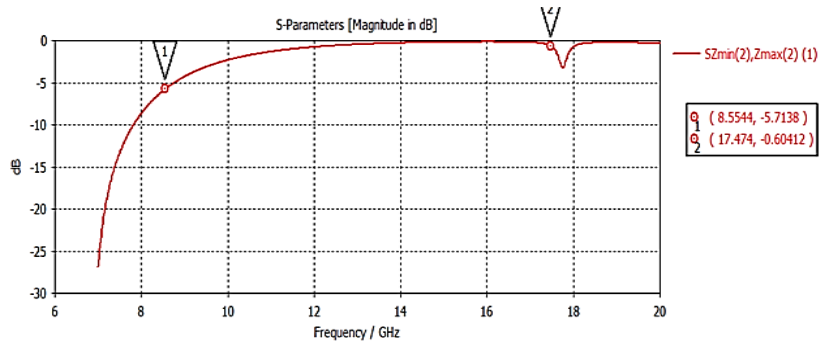


Figure 6: Transmission parameters (pass band) for TE and TM

The proposed FSS is not influenced by polarization because of its symmetrical design, although this aspect is not thoroughly investigated in this study. Since incident waves can come from different directions, it is preferable to have devices that are not affected by angle. As illustrated in Fig.7 and Fig.8 The graph shows the transmission response for both TE mode and TM mode at different incident angles. It is clear that the frequency response of the FSS remains consistent across various incident angles, with the bandstop transmission response staying mostly the same at incident angles below 20 degrees with a reference of -15dB. This indicates that the structure can be used in more complex applications because it is not sensitive to incident angles. Tables 2 show simulation results for both TM and TE polarizations. Similarly, the angular variation from 0° to 20° for the FSS structure in the passband is shown in Fig.9 and Fig. 10.

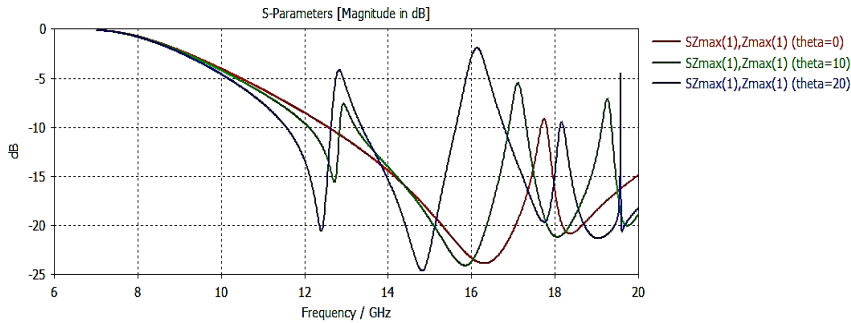


Figure.7. Incidence angle variation of stop band unit cell in TE

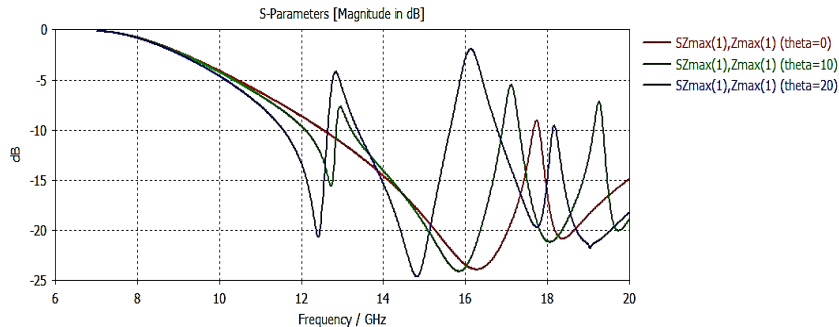


Figure 8. Incidence angle variation of stop band unit cell in TM

Table 2: 10 dB transmission bandwidths 7/20GHz for TE and TM polarization

Angle	TE			TM		
	TE0°	TE10°	TE20°	TM0°	TM10°	TM20°
Resonant frequency fr1 GHZ	16.31	15.85	14.82	16.27	15.85	14.81
Bandwidth BW GHZ	5.019	3.63	2.23	5.00	3.64	2.24

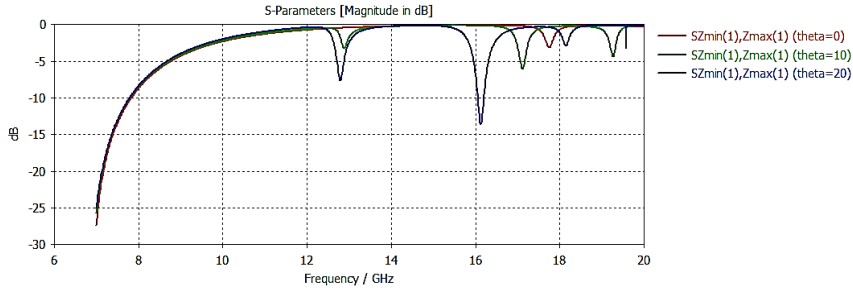


Figure.9. Incidence angle variation of pass band unit cell in TE mode

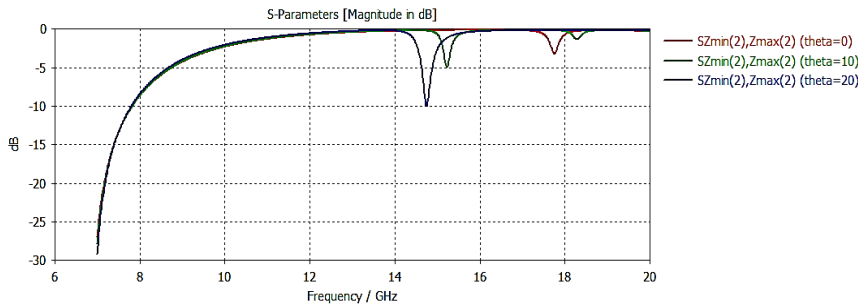


Figure.10 Incidence angle variation of pass band unit cell in TM mode

4. Conclusions

This paper presents a single-layered FSS designed for 6G communication. The FSS consists of a 600 nm thick layer of gear-shaped metallic array deposited on 1 mm thick quartz glass. Simulation results show that the FSS has excellent bandstop filtering capabilities, with a resonant frequency of 16.63GHz and -80dB attenuation. Additionally, the FSS is not affected by polarization or incident angles. A prototype of the FSS was fabricated and its transmission response was measured using free space measurement. The measured results align with the simulated ones, confirming the reliability of the design and fabrication. Due to its simple structure, low cost, and ease of fabrication and integration, the proposed FSS is suitable for bandstop filtering applications, and can enhance communication performance and anti-interference ability in future 6G communication systems

References

- [1]. Mahmoud, H.H.H.; Amer, A.A.; Ismail, T. 6G: A comprehensive survey on technologies, applications, challenges, and research problems. Trans. Emerg. Telecommun. Technol. 2021, 32, e4233.]

- [2]. Zhu, J.; Yang, Y.; Li, M.; Mcgloin, D.; Liao, S.; Nulman, J.; Yamada, M.; Iacopi, F. Additively Manufactured Millimeter-Wave Dual-Band Single-Polarization Shared Aperture Fresnel Zone Plate Metalens Antenna. *IEEE Trans. Antennas Propag.* 2021, 69, 6261–6272.
- [3]. Lin, J.-Y.; Yang, Y.; Wong, S.-W.; Li, Y. High-Order Modes Analysis and Its Applications to Dual-Band Dual-Polarized Filtering Cavity Slot Arrays. *IEEE Trans. Microw. Theory Tech.* 2021, 69, 3084–3092.
- [4]. Li, M.; Yang, Y.; Iacopi, F.; Yamada, M.; Nulman, J. Compact multilayer bandpass filter using low-temperature additively manufacturing solution. *IEEE Trans. Electron. Devices* 2021, 68, 3163–3169.
- [5]. Li, M.; Yang, Y.; Iacopi, F.; Nulman, J.; Chappel-Ram, S. 3D-Printed Low-Profile Single-Substrate Multi-Metal Layer Antennas and Array with Bandwidth Enhancement. *IEEE Access* 2020, 8, 217370–217379.
- [6]. Zhu, J.; Yang, Y.; Chu, C.; Li, S.; Liao, S.; Xue, Q. Low-profile wideband and high-gain LTCC patch antenna array for 60 GHz applications. *IEEE Trans Antennas Propag.* 2020, 68, 3237–3242.
- [7]. Dang, S.; Amin, O.; Shihada, B.; Alouini, M.-S. What should 6G be? *Nat. Electron.* 2020, 3, 20–29.
- [8]. Wang, H.B.; Cheng, Y.J. 140 GHz Frequency Selective Surface Based on Hexagon Substrate Integrated Waveguide Cavity Using Normal PCB Process. *IEEE Antennas Wirel. Propag. Lett.* 2018
- [9]. Shen, Y.; Chen, D.; Wei, Q.; Lin, S.; Shi, L.; Wu, L.; Guo, G. 183 GHz Frequency Selective Surface Using Aligned Eight-layer Microstructure. *IEEE Electron. Device Lett.* 2018, 39, 1612–1615.
- [10]. Poojali, J.; Ray, S.; Pesala, B.; Venkata, K.C.; Arunachalam, K. Quad-Band Polarization-Insensitive Millimeter-Wave Frequency Selective Surface for Remote Sensing. *IEEE Antennas Wirel. Propag. Lett.* 2017, 16, 1796–1799.
- [11]. Das, S.; Reza, K.M.; Habib, A. Frequency Selective Surface Based Bandpass Filter for THz Communication System. *J. Infrared Milli. Terahertz Waves* 2012, 33, 1163–1169
- [12]. Poon, N.H.; Yan, Y.; Zhou, L.; Wang, D.; Chan, C.-H.; Roy, V.A.L. Frequency Selective Surfaces with Nanoparticles Unit Cell. *Micromachines* 2015, 6, 1421–1426
- [13] MARCUVITZ, N. : "Waveguide handbook "(McGraw-Hill , 1951)